# Mixed convection from a rotating horizontal heated cylinder placed in a low-speed wind tunnel

**J. Jones*, D. Poulikakos† and J. Orozco‡**
Department of Mechanical Engineering, University of Illinois at Chicago, Chicago, IL 60680, USA

*Received 7 July 1987 and accepted for publication 1 October 1987*

Combined forced and natural convection from a rotating horizontal heated cylinder placed in a low-speed wind tunnel is investigated through numerous experiments set in the counterflow arrangement, i.e., with the free-stream velocity directed parallel to the gravity vector and opposite to the natural convection flow. The main goal of this work is to determine the dependence of the overall heat flux from the rotating cylinder, represented by the Nusselt number, on the free-stream Reynolds number, the rotational Reynolds number, and the Rayleigh number. Several correlations documenting this dependence were obtained and are presented in this paper. Good agreement with former investigations for several limiting cases is found and discussed. Scaling analysis, accurate in an order of magnitude sense, is also applied to define approximately the regions of dominance of the three heat transfer mechanisms involved in the problem: natural convection, free-stream forced convection, and rotational forced convection.

**Keywords:** experimental mixed convection; rotating heated cylinder; low-speed wind tunnel; forced convection; rotating flow

## Introduction

Heat transfer from a rotating solid to a moving fluid has attracted the attention of researchers over the past several decades, because of its numerous applications in thermal engineering, ranging from the cooling of rotating machinery and reentry space vehicles, to the paper industry. Drying paper on rollers accounts for a large percentage of the total energy consumption in the paper industry.

The present study focuses on the problem of mixed convection from a horizontal rotating heated cylinder placed in a low-speed wind tunnel. The flow in the wind tunnel is directed parallel to gravity. The main goal of the present research is to determine the dependence of the overall heat transfer from the cylinder, represented by the Nusselt number, on the free-stream Reynolds number, the rotational Reynolds number, and the Rayleigh number.

The convection phenomenon from the heated cylinder is governed by three interweaving mechanisms: forced convection due to the wind tunnel, forced convection due to rotation, and natural convection. Each mechanism, any combination of two mechanisms, or all three mechanisms together may be mainly responsible for the cooling of the heated cylinder. Clearly, then, there exist seven possible types (regimes) of convective heat transfer, and the difficulties of obtaining accurate correlations for the Nusselt number are formidable.

Published correlations exist for several of the above regimes for certain ranges of the problem parameters (the two Reynolds numbers and the Rayleigh number). For laminar flow natural convection from a stationary isothermal cylinder placed in a quiescent fluid, Dorfman[1] and Etemad[2] found that

$$\mathrm{Nu}=0.456\mathrm{Ra}^{0.25}, \qquad 10^5<\mathrm{Ra}<10^6 \tag{1}$$

For turbulent natural convection Equation 1 becomes[3]

$$\mathrm{Nu}=0.14\mathrm{Ra}^{0.33}, \qquad \mathrm{Ra}>10^8 \tag{2}$$

A more general correlation for the same problem was proposed later by Churchill and Chu[4]. Interesting results for the flow and temperature field as well as the overall and local heat transfer from an isothermal horizontal heated cylinder cooled by natural convection were obtained by Kuehn and Goldstein[5].

Numerous correlations exist in the literature for the problem of forced convection from a stationary isothermal or constant-heat-flux cylinder[3,6-8]. By comparing the published correlations for this problem, one cannot help but notice the disagreement in the leading coefficient and the power of the independent variable. For example Morgan's[8] and Ahmad's[6] correlations for the same problem, are, respectively,

$$\mathrm{Nu}=0.148\mathrm{Re}^{0.633}, \qquad 6.8\times10^3<\mathrm{Re}<2.2\times10^4 \tag{3}$$

$$\mathrm{Nu}=0.0675\mathrm{Re}^{0.773}, \qquad 5\times10^3<\mathrm{Re}<5\times10^4 \tag{4}$$

When rotation is present in the system, the existing results are considerably less conclusive. When forced convection due to rotation alone dominates the heat transfer (natural convection and forced convection due to the incoming flow are neglected), Anderson and Saunders[9], and later Dropkin and Carmi[10] and Etemad[2], proposed correlations for the Nusselt number. The main difference between the correlations proposed in Ref. 9 relative to the correlation proposed in Refs. 2 and 10 is the exponent of $\mathrm{Re}_\omega$. More specifically, Anderson and Saunders[9] claimed that $\mathrm{Nu}\sim\mathrm{Re}_\omega^{2/3}$, after they used an ad hoc argument, which they said was inexact. The experiments in Refs. 2 and 10 showed that $\mathrm{Nu}\sim\mathrm{Re}_\omega^{0.7}$.

* Graduate Student.
† Associate Professor.
‡ Assistant Professor.

Dennis and Badr[11] examined numerically the problem of forced convection due to the combined effect of rotation and free-stream flow field (natural convection was neglected). They postulated that the nature of heat transfer depends drastically on the ratio of the two Reynolds numbers involved, and they felt that it is unlikely that a single correlation would be able to give satisfactory results for all possible ranges of Reynolds numbers.

The effect of natural convection on the heat transfer from a stationary cylinder in crossflow was studied by Ahmad[6]. He was not able to propose a correlation that would conclusively document the mixed convection regime, even though his study shed light on several aspects of the problem. A correlation for the problem of combined forced rotational-natural convection holding for relatively low Rayleigh numbers was reported by Etemad[2]. Temperature and flow field results for the same problem have been published by Farouk and Ball[12].

The least amount of work has been performed for the case where all three heat transfer mechanisms (rotational forced convection, free-stream forced convection, and natural convection) are present. The most reliable correlation for the Nusselt number was proposed by Kays and Bjorklund[13] and was tested successfully by the General Electric Company[14]. However, this correlation is accurate only when the effect of natural convection is marginal.

In summary, after reviewing the existing correlations for the Nusselt number in the literature, it became apparent that a considerable amount of work is needed to document the regimes in which the contribution of natural convection to free-stream forced convection, or to rotational forced convection, or to both simultaneously, is significant. Therefore, this is the main purpose of this work. In addition, it verifies and extends the range of validity of results from previous investigations.

## Experimental apparatus

### *The wind tunnel*

A low-velocity open-circuit wind tunnel constructed at the University of Illinois at Chicago[6] was used for the experiments. Standing about 4 m tall in (axial) length, it tapers from 0.965 $m^2$ at its mouth to 0.38 $m^2$ at the Plexiglas test section to give a contraction ratio of 6.45 (ratio of the two respective areas). The frame was constructed to rotate up to 360° so that any flow direction dependencies (such as those that occur in mixed convection) could be studied. In this experiment, the direction of the airflow was oriented downward toward the earth to oppose the natural convection plume and thus produce a "counterflow."

Uniform flow was ensured through its range of 0–10 m/s by three wire crosshatched screens and a honeycomb mesh located in the expandable section of the entrance. Velocity was taken slightly upstream of the rotating cylinder to avoid its inadvertently affecting the measurement. No significant variation in the flow field could be measured by these investigators. A suction fan was operated by a belt-and-pulley, 2-hp variable-speed DC motor. Such a strong motor creates a rather strong airflow, with Reynolds numbers up to 35,000; at its lowest setting the free-stream Reynolds number is already as high as 1300. No further details on the wind tunnel are given here, for they can be found in Ref. 6.

Free-stream velocities inside the wind tunnel were measured with a DISA Electronics Company hot wire anemometer. Calibration is necessary because each device will operate differently under different conditions. The hot wire was calibrated by interpreting manometer pressure measurements via the Bernoulli equation through the range of wind tunnel speeds and interpolating the corresponding hot wire voltage readings numerically via a curve-fit computer program developed and tested successfully at the Argonne National Laboratory. The relationship between hot wire voltage and wind tunnel velocities is very close to a fourth-degree polynomial.

### *The rotating cylinder*

A 54-mm O.D. piece of standard copper tubing 1.6 mm thick and 351 mm long (Figure 1a) was rotated inside the wind tunnel test section. Extra light two-shield bearings were used at both ends mounted into the Plexiglas test section walls, leaving approximately 3.2-mm clearance between them and the rotating cylinder. A 305-mm-long, 14.4-Ω cylindrically shaped resistance heater was mounted in the center of the copper tubing; the gap

## Notation

| | |
|---|---|
| $D$ | Cylinder diameter, m |
| $g$ | Gravitational acceleration, $m/s^2$ |
| Gr | Grashof number, $g\beta\Delta TD^3/\nu^2$ |
| $h$ | Overall heat transfer coefficient, $W/m^2K$ |
| $k$ | Air thermal conductivity, W/mK |
| $L$ | Cylinder length, m |
| Nu | Overall Nusselt number, $hD/k$ or $Q/(T_w - T_\infty)\pi Lk$ |
| Pr | Prandtl number, $\nu/\alpha$ |
| $Q$ | Power, W |
| $q$ | Heat flux, $W/m^2$ |
| Ra | Rayleigh number based on the cylinder diameter and the wall to free-stream temperature difference, $[g\beta(T_w - T_\infty)D^3]/\nu\alpha$ |
| $Ra_*$ | Rayleigh number based on the heat flux from the cylinder and the diameter of the cylinder, $g\beta qD^4/k\nu\alpha$ |
| Re | Free-stream Reynolds number, $DU_\infty/\nu$ |
| $Re_\omega$ | Rotational Reynolds number, $D^2\omega/2\nu$ |
| rpm | Revolutions per minute |
| $T_w$ | Cylinder wall temperature |
| $T_\infty$ | Free-stream air temperature, K |
| $u$ | Velocity component in the $x$-direction |
| $U_\infty$ | Free-stream air velocity, m/s |
| $v$ | Velocity component in the $y$-direction |
| $x$ | Coordinate parallel to the surface |
| $y$ | Coordinate perpendicular to the surface |

*Greek letters*

| | |
|---|---|
| $\alpha$ | Air thermal diffusivity, $m^2/s$ |
| $\beta$ | Air coefficient of thermal expansion |
| $\delta_{NC}$ | Boundary layer thickness scale for natural convection |
| $\delta_{FC}$ | Boundary layer thickness scale for free-stream forced convection |
| $\delta_{RC}$ | Boundary layer thickness scale for rotational forced convection |
| $\theta$ | Angle |
| $\nu$ | Air kinematic viscosity, $m^2/s$ |
| $\rho$ | Air density, $kg/m^3$ |
| $\omega$ | Cylinder angular velocity, $s^{-1}$ |

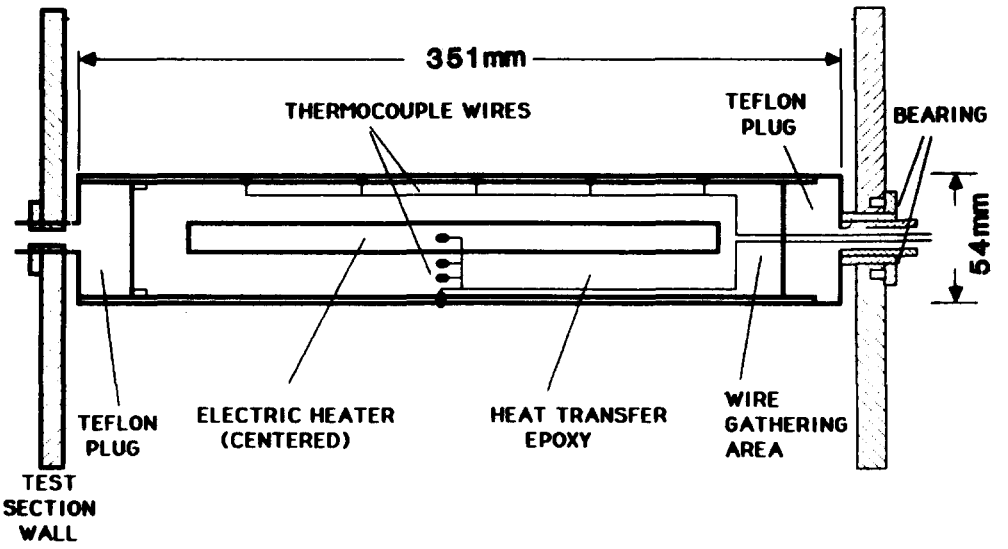


*Figure 1* (a) Schematic of the cross section of the rotating cylinder

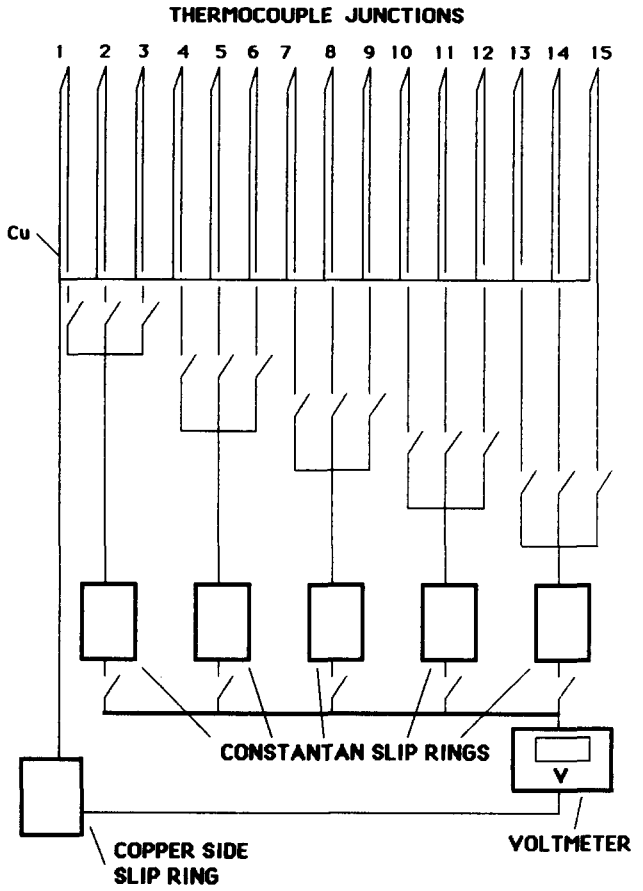


*Figure 1* (b) the thermocouple switching arrangement

between the heater and the copper tubing was filled with Thermon Co. T-63 heavy-duty heat transfer cement. The entire apparatus was cured for three days at 27°C to drive off air bubbles from the heat transfer cement during the construction of the apparatus. To ensure the minimum possible heat loss through the sides of the cylinder (to reduce "end effects"), asbestos caps were placed next to the heater and the copper tubing was sealed at the ends with 12.7-mm Teflon plugs. At no time did the bearings or the Plexiglas walls of the test section get hot to the touch, indicating that end effects were effectively minimized, for the range of the present experiments ($Nu \sim 20$–30). However, for larger Nusselt numbers in forced convection ($Nu \sim 150$) the end effect, even though still small, could introduce an error of about 5%. In addition, thermal radiation losses were negligible because the surface of the cylinder was highly polished and its temperature sufficiently low.

The cylinder was rotated by an externally connected shaft using a pulley drive system powered by a variable-speed DC motor. For better control of the device at low rpm's, the input power line to the motor was connected to an AC variac. Two drive pulleys and belts were constructed to allow the device to rotate up to 5000 rpm. Vibration control consisted of an adjustable set screw (weighted) mounting that could be moved in or out to offset any imbalance in the roundness of the apparatus. Balanced as constructed, it turns at 2000 rpm without problems.

Below 50 rpm, rotation was observed by the stopwatch timing method, and the Variac was adjusted to 1% rpm accuracy. At rotations above 50 rpm, a Strobotac (strobe) light was used to adjust the angular rotation to 0.1% accuracy. The measurement of rotational speed added a maximum of 0.5% relative error to the total experimental error. In most cases this relative error was actually much less.

At the end of the drive shaft a cylindrically shaped housing was mounted for the electronics and the thermocouple-wire switching apparatus. Mounted along the drive shaft were the power slip rings for supplying current to the heater and the instrumentation slip rings for reading thermocouple measurements.

Direct current was supplied to the resistance heater from a Hewlett-Packard 6422C power supply, whose current output was verified through a Weston Instruments ammeter. The power input to the heater was calculated by multiplying the voltage across the heater by the current through the heater.

### *The temperature measurement arrangement*

Copper-constantan type T thermocouples were used to make temperature measurements in the experiments. Fourteen holes were drilled in the copper tubing, seven each along a single axial

line, and eight around a circle located in the center of the test section 45° apart from each other. The thermocouple beads were fixed in place with small amounts of copper oxide cement, and the wires were cemented in place. The thermocouple leads were run out through the center of the copper tubing, through the center of one of the sidewall bearings, through the center of the drive shaft to the electronics switching housing at the end of the assembly next to the wind tunnel test section. A fortunate advantage of using this wiring scheme was the natural noise shielding of the thermocouple circuit.

The thermocouple output voltages were sent through instrumentation slip rings. The cost of measuring cylinder temperatures was minimized by using a six-slip-ring apparatus, which allowed five concurrent thermocouple measurements. This was achieved through an electrical circuit conceived, designed, and built in our laboratory. The basic idea was to have a common wire for all the copper-side thermocouple leads and to use a switching scheme with groups of three leads each on the constantan side. The switches were soldered into place after heavily binding them inside the housing; they withstood the 2000-rpm test. The slip ring leads were then connected once again to copper and constantan, respectively, which produced a complete thermocouple circuit when connected to an ice-bath reference junction. Temperatures were measured with an HP 3467A digital multimeter. Figure 1(b) is a diagram of the thermocouple switching arrangement.

An important issue that had to be investigated was the rotational limit of the device imposed by the error introduced to the temperature measurements because of the rotation. By letting the device run at various rotational speeds and measuring the voltage introduced by the slip ring junction heating over and above that of the room temperature reading, we determined that 500 rpm was the physical reliable limit of this device. Above 500 rpm, the thermally introduced voltage increased rapidly, until, at 750 rpm, noise affected the output voltage, which fluctuated significantly so that the cylinder temperature could not be determined accurately.

The total relative error of the experimental measurements (free-stream velocity, power to the heater, and temperature) was estimated to be less than 5%.

## Results and discussion

All told, 541 experiments were run, 346 of which with a crossflow of air directed downward opposed to the gravity vector, the remainder without the wind tunnel effect. The experiments were conducted in such a way that a wide range of each of the three independent variables—Ra, Re, and $\mathrm{Re}_\omega$—was explored given the physical limitations of this apparatus. The wind tunnel was run through its entire range, although the majority of points were taken at its lowest settings; the rotational speed was run up to the physical limit of the temperature sensing device (500 rpm); the cylinder was heated to over 200°C in order to obtain consistently higher Rayleigh numbers than have been heretofore presented in the literature. The findings are presented as a series of two-dimensional graphs; the heat transfer (represented by the Nusselt number) is, however, a function of three independent dimensionless parameters. Much insight can be gained into the problem by fixing two of the independent variables involved and determining the behavior of Nu when the third parameter is varied. Further understanding can be gained from analysis of the heat transfer by studying the regions in which only one of the three independent nondimensional variables is dominant (the "asymptotes" of the solution) by discovering the limits to those regions and comparing them to existing correlations.

To determine the regions in which a unique heat transfer mechanism is dominant, a scaling analysis of the governing conservation equations was performed. This analysis is accurate in an order of magnitude sense. All the details of the scaling analysis are reported in Ref. 15. Scaling analysis has been applied to several basic heat transfer problems in a recent convective heat transfer textbook[16]. The key steps of the scaling analysis are reported in the appendix. The Boussinesq-incompressible governing equations used for the scaling analysis were written with respect to a curvilinear coordinate system measuring along and perpendicular to the cylinder surface. No variations in the axial direction were taken into account. In addition, the equations used were for laminar flow, even though the flow around the cylinder was turbulent for our experiments. Despite these drawbacks, it is believed that the regimes defined by the scaling analysis are "conservative" and much less heuristic than what is reported in the literature[6,9,17]. The final results of the scaling analysis are the order of magnitude estimates of the thermal boundary layers when natural convection dominates,

$$\delta_{\mathrm{NC}}/D \sim \mathrm{Ra}^{-1/4} \tag{5}$$

when free-stream forced convection dominates,

$$\delta_{FC}/D \sim \mathrm{Pr}^{-1/2}\mathrm{Re}^{-1/2} \tag{6}$$

and when rotational forced convection dominates,

$$\delta_{\mathrm{RC}}/D \sim \mathrm{Pr}^{-1/2}\mathrm{Re}_\omega^{-1/2} \tag{7}$$

Clearly, a criterion dictating when a heat transfer mechanism dominates over another is obtained if the scales of the thermal boundary layers of two mechanisms are compared. For example, if the thermal boundary layer scale of natural convection is smaller (in an order of magnitude sense) than the scale of rotational forced convection, the heat transfer from the rotating cylinder is dominated by natural convection. Based on the above, the following regions are defined:

(a) Natural convection dominates over rotational forced convection:

$$\mathrm{Ra}^{-1/4} \ll \mathrm{Pr}^{-1/2}\mathrm{Re}_\omega^{-1/2} \tag{8}$$

(b) Natural convection dominates over free-stream forced convection:

$$\mathrm{Ra}^{-1/4} \ll \mathrm{Pr}^{-1/2}\mathrm{Re}^{-1/2} \tag{9}$$

(c) Free-stream forced convection dominates over rotational forced convection:

$$\mathrm{Re}^{-1/2} \ll \mathrm{Re}_\omega^{-1/2} \tag{10}$$

The criteria outlined above will serve to categorize the experimental data. At first, the regimes in which a single heat transfer mechanism is dominant were examined. Figure 2(a) shows the dependence of Nu on Re for $\mathrm{Re} > 3000$. The experimental points shown in this figure were selected out of the total amount of data points by using criteria (9) and (10) to define the region where free-stream forced convection dominates. Since inequalities (8)–(10) are accurate in an order of magnitude sense, we decided to use them throughout the study by defining the symbol "$\gg$" to mean "at least twice as large." For example, based on the above convection, for every point in Figure 2(a), $\mathrm{Ra}^{-1/4}$ is at least twice as large as $\mathrm{Pr}^{-1/2}\mathrm{Re}^{-1/2}$ and $\mathrm{Re}_\omega^{-1/2}$ is at least twice as large as $\mathrm{Re}^{-1/2}$. The upper solid line represents the correlation proposed in Ref. 6 for forced convection from a stationary cylinder. The lower line represents a correlation proposed in Ref. 8 for the same problem. The correlations in Refs. 6 and 8 represent the upper and lower limits of existing correlations in the literature for forced convection from a stationary cylinder. Clearly, our experimental data agree

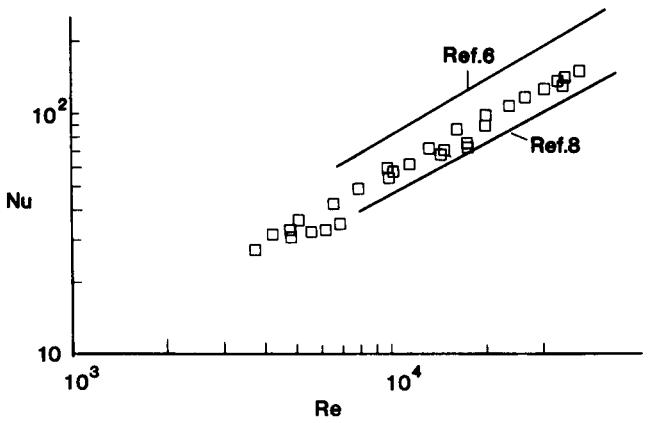


*Figure 2(a)* Nusselt number versus Re in the regime where the free-stream forced convection is dominant: $Pr^{1/2}Re^{1/2}/Ra^{1/4} > 2$ and $Re^{1/2}/Re_\omega^{1/2} > 2$

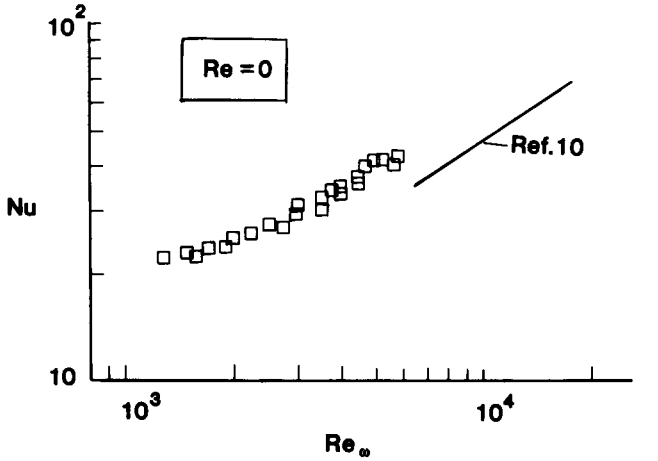


*Figure 2(b)* Nusselt number versus $Re_\omega$ for $Pr^{1/2}Re_\omega^{1/2}/Re^{1/4} > 2$ and Re=0

well with the published results, and, therefore, criteria (9) and (10) determine correctly the points for which forced convection in dominant. Our experimental data in Figure 2(a) are correlated by

$$Nu = 0.046Re^{0.76} \tag{11}$$

Next, the case where the heat transfer was dominated by rotational forced convection was examined. Because of the limitation of the apparatus to 500 rpm, the rotational forced convection asymptote was not reached exactly. Figure 2(b) shows that the trend revealed by the experimental data implies that the forced convection asymptote would be reached at higher rpm. A rotational Reynolds number of over 10,000 is necessary to dominate the natural convection effect. Our experiments for the most part did not exceed $Re_\omega = 5000$. The points in Figure 2(b) are for Re=0 and were selected with the help of criterion (8). These points are correlated by

$$Nu = 0.5Re_\omega^{0.5} \tag{12}$$

For very slow rotation it is suggested[14] that the results for Nu for stationary cylinders are used. To investigate the correctness of this approximation, we carried out a series of experimental runs for very slow rotation (2 rpm, $Re_\omega = 25$) with the wind tunnel off. The data, which satisfy criterion (8), were correlated by

$$Nu = 0.2Ra^{1/3} \tag{13}$$

Figure 3 compares the experimental data with a correlation proposed by Dorfman[1] for natural convection from a stationary cylinder. Clearly, the rotation augments heat transfer. Another important conclusion can be drawn by examining correlation (13) and Figure 3. The dependence of Nu on Ra is identical to that of turbulent natural convection from a horizontal cylinder of diameter $D$, even though the range of Ra in Figure 3 ($10^6 < Ra < 10^7$) corresponds to laminar natural convection from a horizontal cylinder ($Ra > 10^9$ is required for turbulent natural convection). Therefore, the existence of slow rotation enhances the heat transfer. One may speculate that viscous forces acting in the fluid due to the rotation cause mixing of the fluid and augment heat transport in a way similar to turbulence. Increasing $Re_\omega$ in the region where natural convection dominates yielded similar results. For example, for $Re_\omega = 1000$ and Re=0,

$$Nu = 0.27Ra^{0.31}, \qquad 10^6 < Ra < 4 \times 10^6 \tag{14}$$

Comparing correlations (13) and (14), we clearly see that the effect of natural convection is dominant: increasing $Re_\omega$ drastically had only a slight effect on reducing the exponent of Ra in Nu correlations.

Next, the dependence of Nu on the problem parameters was determined when both natural convection and rotational forced convection or all three mechanisms affected the heat transfer. The regimes of natural convection, free-stream forced convection, and rotational forced convection have been researched quite extensively by previous investigators[6-8,13,14,18].

## *Mixed natural convection and rotational forced convection*

Throughout the experiments that aimed to investigate the mixed natural convection and rotational forced convection regime, the wind tunnel was off (Re=0). Figure 4 illustrates the effect of the rotational Reynolds number ($Re_\omega$) on Nu. At slow rotational speeds the heat transfer from the cylnder is nearly independent of $Re_\omega$. At $Re_\omega \approx 1500$ the rotation begins to affect the convection process, and as $Re_\omega$ increases, the rotational forced convection asymptote is approached. The transition region is predicted correctly (in an order of magnitude sense by the scaling Equation (8)). Clearly, the transition region depends on

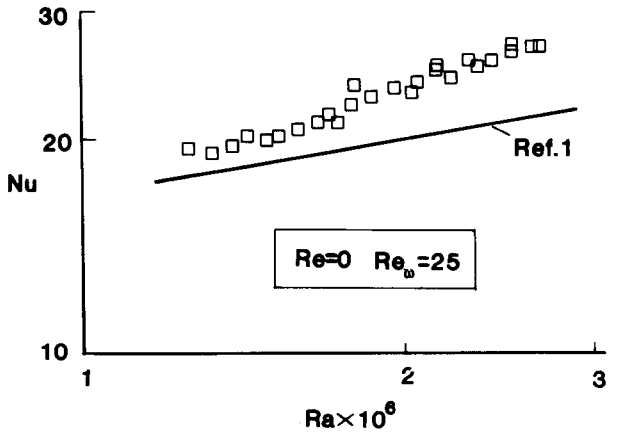


*Figure 3* Nusselt number versus Ra for slow rotation ($Re_\omega$=25) and Re=0

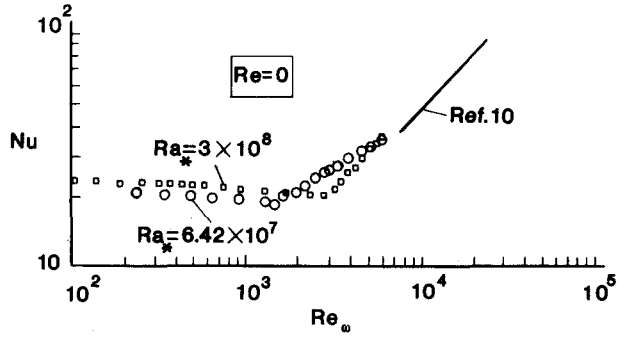


*Figure 4* Nusselt number versus $Re_\omega$ for Re=0, illustrating the transition region from natural convection to rotational forced convection

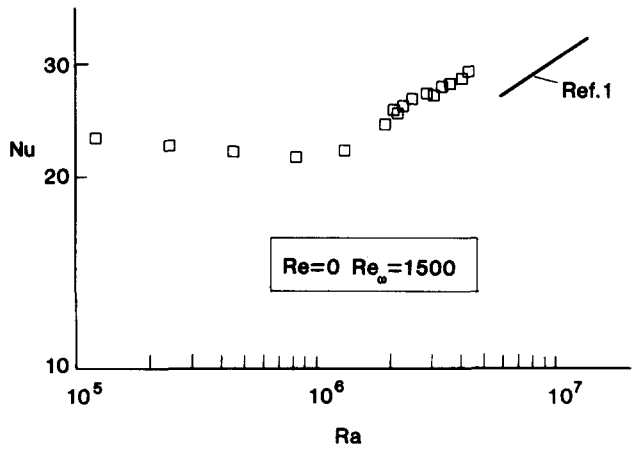


*Figure 5* Nusselt number versus Ra for Re=0, illustrating the transition region from rotational forced convection to natural convection

the heat input to the cylinder. Increasing $Ra_*$ increases the value of $Re_\omega$ at which rotation seriously affects the heat transfer.

Next, if one focuses on the transition region, a slight dip in the Nusselt number values is observed before the rotational forced convection takes over and starts dominating the heat transfer. This phenomenon was also observed and discussed in passing by Etemad[2] but not by Farouk and Ball[12], who never observed its existence. The slight decrease in Nu with increasing $Re_\omega$ in the transition region is an important finding, for it implies that the effect of rotation in this region when combined with natural convection is likely to deteriorate, rather than augment, heat transfer. A similar dip in the value of Nu has been observed (for different reasons) in turbulent mixed convection in vertical tubes and in hot wire anemometry[20] when mixed convection occurs.

Figure 5 shows the transition from rotational forced convection to natural convection. This time $Re_\omega = 1500$ is fixed. The similarity between Figures 4 and 5 is clear, with the roles of $Re_\omega$ and Ra reversed: the lack of Ra dependence in the low Ra range, the slight dip in heat transfer early in the transition region, and the growing dominance of natural convection as Ra increases. The natural convection asymptote is included in Figure 5 to illustrate the point that this asymptote is very likely to be approached at even higher values of Ra.

Figure 6 shows the effect of rotation on Nu when the natural convection mechanism does not dominate the heat transfer. A 20% (approximately) increase in heat transfer for natural convection from a slowly rotating cylinder is observed relative to the case of natural convection from a stationary cylinder. The slope of the line for the rotational case is similar to the slope of the line for the stationary case.

Additional experiments indicated that increasing the rotation increased the heat transfer, past a certain critical value of $Re_\omega$, until the rotational forced convection asymptote was approached (Figure 7). The findings presented in Figure 7 indicate a rather smooth transition between natural convection and rotational forced convection and agree with the results of Anderson and Saunders[9]. On the other hand, our results contradict Ref. 12, which implied that a sharp transition takes place after which rotational convection dominates. Only 12 experiments were run in Ref. 12, and not enough attention was focused on obtaining sufficient data in the transition region.

### *Combined natural, rotational, and free-stream convection*

Figure 8 shows the effect of Re on Nu at a low $R_\omega$ and high Ra. The dependence of Nu on Re is not monotonic. The heat transfer becomes minimal for a certain value of Re. The reason for this important finding is speculated as follows. Since in the counterflow arrangement the free-stream flow is opposing the buoyant plume rising from the cylinder, a certain critical free-stream Reynolds number exists, beyond which the free-stream flow starts dominating the heat transfer. On the other hand,

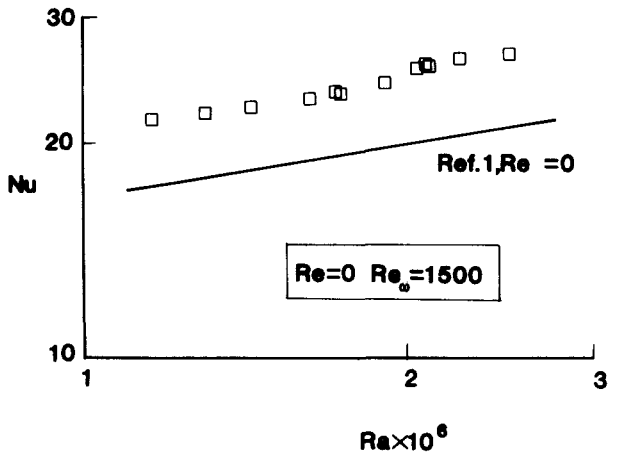


*Figure 6* Nusselt number versus Ra for a rotational speed in the transition region ($Re_\omega$=1500) and for Re=0

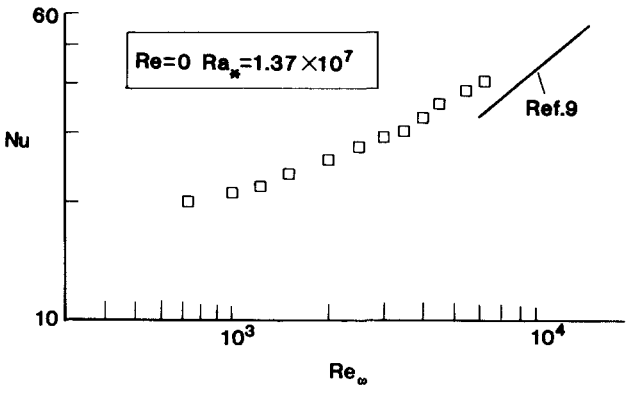


*Figure 7* Nusselt number versus $Re_\omega$ in the transition region for $Ra_* = 1.37 \times 10^7$ and Re=0

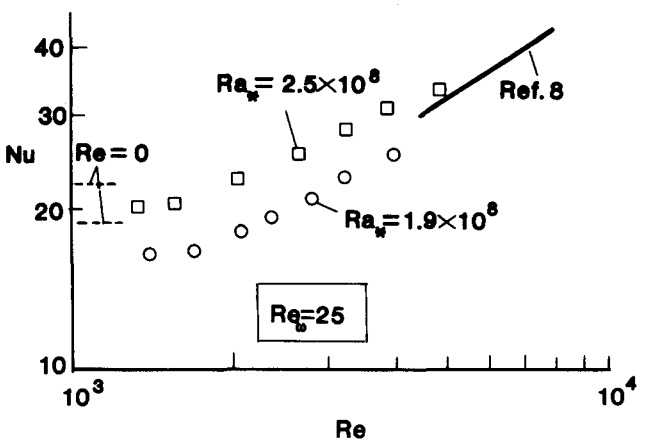


*Figure 8* Nusselt number versus Re for a slow rotation ($Re_\omega = 25$) and for two values of $Ra_*$

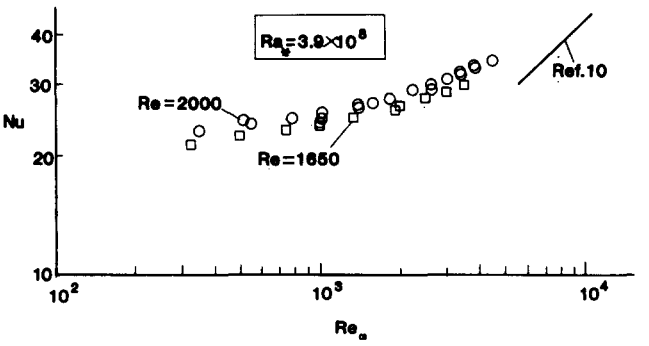


*Figure 9* Nusselt number versus $Re_\omega$ for $Ra_* = 3.9 \times 10^8$ and Re = 1650 and Re = 2000

when the value of Re is much smaller than the critical Re, the heat transfer is dominated by natural convection and the free-stream, flow has a hindering effect on the cooling of the cylinder. This nonmonotonic behavior is a typical example of the complex interactions involved in the problem under investigation. These interactions are largely ignored in the mixed convection correlations in the literature, which are all monotonic.

Next, the effect of the free-stream flow on the transition from natural convection to rotational forced convection, discussed in connection with Figure 4, was investigated. As shown in Figure 9, adding the free-stream flow to the picture changes the "transition points" where one effect becomes dominant over the other as well as the slope of the Nu-$Ra_\omega$ curve. For Re = 1650 the transition region is extending over a wider range of $Re_\omega$ and the dominance of rotational convection takes place at higher values of $Re_\omega$ (well outside the range of our apparatus) compared with the Re = 0 case (Figure 4). Increasing Re to 2000 has the same qualitative effect.

Another interesting observation is that the dip in the Nusselt number graph observed in the transition region for Re = 0 (Figure 4) was not observed for Re = 1650 or 2000. Finally, a general qualitative result from the experiments involving the three heat transfer mechanisms all together in the mixed convection region is that the effect of one of the three heat transfer mechanisms on Nu when the other two mechanisms are present is less drastic compared with the effect of the same mechanism on Nu in the absence of the other two mechanisms.

### *Proposed correlations*

Kays and Bjorklund[13] have proposed the following correlation for the mixed convection regime:

$$Nu = 0.135[(Re_\omega^2/2 + Re^2 + Gr)Pr]^{1/3} \quad (15)$$

This correlation agreed well with our experimental data when natural convection was not significant. It performed best when the convection phenomenon was dominated by the wind tunnel. Figure 10 shows the present experimental points plotted against Equation 15. The triangular symbols correspond to Re = 0, and they disagree the most with the correlation. Due to the limitations of our wind tunnel (size of the motor driving the fan), once the wind tunnel was on, free-stream forced convection was already sizable. The agreement between our experiments and the correlation is best in the upper right region of the graph, representing higher Re. Clearly, the lower left region of the graph needs serious improvement, and it represents the points where natural convection was significant.

In the absence of free-stream forced convection (Re = 0), Etemad[2] claimed that Nu dependence on Ra and $Re_\omega$ is

$$Nu = 0.11[(Re_\omega^2/2 + Gr)Pr]^{0.35} \quad (16)$$

This relation was proved to perform well for rotation-dominated flows[2], i.e., when the contribution of Gr to the quantity in brackets in Equation 16 is small. Our experiments were performed in the high Ra regime (about two orders of magnitude higher than that of Refs. 2 and 13). Clearly, Figure 11 shows that Equation 16 does not correlate the data satisfactorily in the high Ra regime.

It appears then that a new correlation needs to be proposed to account correctly for the effect of natural convection when this effect is not marginal. This correlation should reduce (at least approximately) to the correlation for turbulence natural convection from a horizontal cylinder when $Re = Re_\omega = 0$. With the help of a curve-fit program, our data yielded the following correlation:

$$Nu = 0.1[Re^2 + Re_\omega^2 + 2Ra]^{0.36} \quad (17)$$

When Re = 0 (no free-stream forced convection) Equation 17 becomes

$$Nu = 0.1[Re_\omega^2 + 2Ra]^{0.36} \quad (18)$$

Figures 12 and 13 prove that correlations (17) and (18) represent a sound improvement over correlations (15) and (16) when natural convection is significant. In addition, they perform as well in the regions of domination of free-stream forced convection and rotational forced convection.

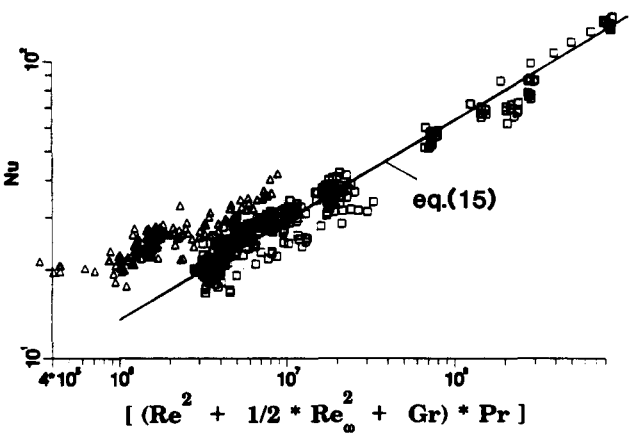


*Figure 10* The data points of the present study, correlated by Equation 15

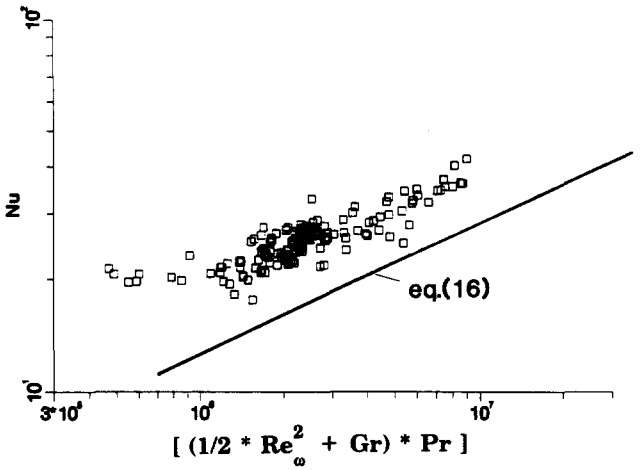


*Figure 11* The data points of the present study for Re=0, correlated by Equation 16

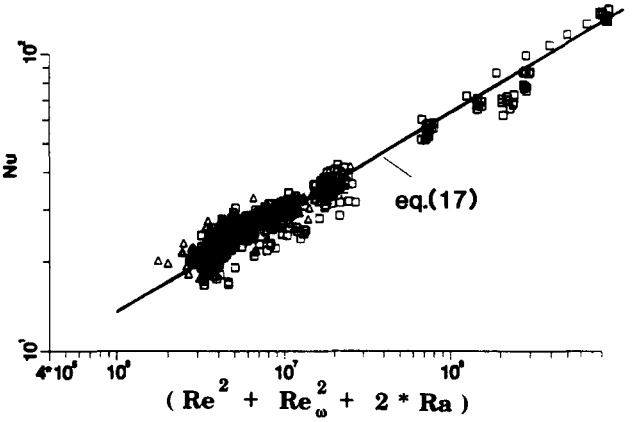


*Figure 12* The data points of the present study correlated by Equation 17

## Conclusion

This paper presented an experimental study of mixed convection from a rotating horizontal heated cylinder placed in a wind tunnel. The focus was on the effect of the three types of convective heat transfer, namely, natural convection, rotational forced convection, and free-stream forced convection on the overall heat flux from the cylinder, represented by the Nusselt number. Throughout the experimental study a reasonably wide range of the problem independent parameters was covered: $0<Ra<10^8$, $0<Re<35{,}000$, and $0<Re_\omega<5000$. Interesting results were obtained for the transition regions between natural convection and one of the two forced convection mechanisms. These results indicate the complexity of the heat transfer phenomenon. For example, in the high Ra regime the transition from natural convection to rotational forced convection is rather smooth and highlighted by a small drop in the value of Nu before rotational forced convection takes over. Adding the free-stream flow has the effect of smoothening further and widening the transition region. For a fixed low value of $Re_\omega$ and for a fixed high value of $Ra_*$, it was found that a weak free-stream flow will decrease Nu until a minimum is reached. Thereafter Nu increases monotonically with Re. In addition, when a slow rotation was superposed to natural convection, a heat transfer enhancement was observed. This enhancement

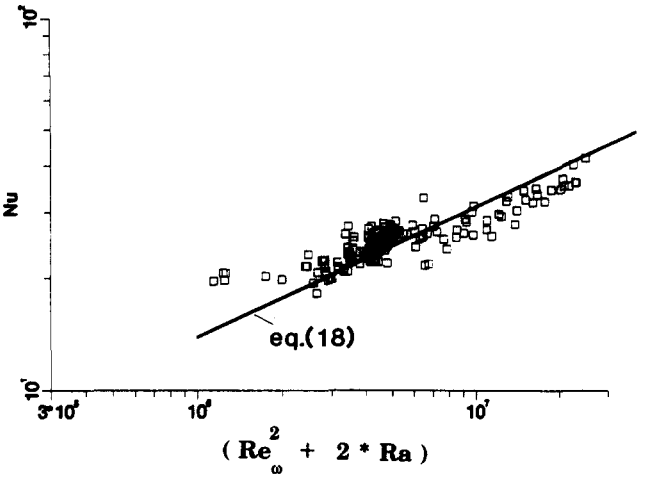


*Figure 13* The data points of the present study for Re=0, correlated by Equation 18

was rather insensitive to the rotational speed for values of $Re_\omega$ less than those in the transition region.

Useful correlations were obtained for Nu dependence on Re, Ra, and $Re_\omega$ or on Ra and $Re_\omega$. These correlations performed well when the heat transfer was seriously affected by natural convection in addition to predicting the dependence of Nu correctly on the problem parameters for flows dominated by rotational forced convection or free-stream forced convection.

## Acknowledgment

Support for this work provided by NSF through grant no. CBT-8451144 is greatly appreciated.

## References

1 Dorfman, L. A. and Serazetdinov, A. Z. Laminar flow and heat transfer near a rotating axisymmetric surface. *Int. J. Heat Mass Transfer*, 1965, **8**, 317–327

2 Etemad, G. A. Free convection heat transfer from a rotating horizontal cylinder to ambient air with interferometric study of flow. ASME Annual Meeting, New York, 1954, Paper No. 54-A-74

3 Holman, J. P. *Heat Transfer*, McGraw-Hill, New York, 1986

4 Churchill, S. W. and Chu, H. H. S. Correlating equations for laminar and turbulent free convection for a horizontal cylinder. *Int. J. Heat Mass Transfer*, 1975, **18**, 1049–1053

5 Kuehn, T. H. and Goldstein, R. J. Numerical solution to the Navier-Stokes equations for laminar natural convection about a horizontal isothermal circular cylinder. *Int. J. Heat Mass Transfer*, 1980, **23**, 971–979

6 Ahmad, R. Mixed convection around a horizontal cylinder. Ph.D. Thesis, University of Illinois at Chicago, 1985

7 Dennis, S. C. R., Hudson, J. D., and Smith, N. Steady laminar forced convection from a circular cylinder at low Reynolds numbers. *Phys. Fluids*, 1968, **11**, 933–940

8 Morgan, V. T. The overall convective heat transfer from smooth circular cylinders. In *Advances in Heat Transfer*, Vol. 11, Academic Press, New York, 1975

9 Anderson, J. T. and Saunders, O. A. Convection from an isolated heated horizontal cylinder rotating about its axis. *Proc. Roy. Soc.*, 1953, **217**, 555–562

10 Dropkin, D. and Carmi, A. Natural convection heat transfer from a rotating horizontal cylinder rotating in air. *Trans. ASME*, 1957, **77**, 741–749

11 Badr, H. M. and Dennis, S. C. R. Laminar forced convection

from a rotating cylinder. *Int. J. Heat Mass Transfer*, 1985, **28**, 253–264
12 Farouk, B. and Ball, K. S. Convective flows around a rotating isothermal cylinder. *Int. J. Heat Mass Transfer*, 1985, **28**, 1921–1935
13 Kays, W. M. and Bjorklund, I. S. Heat transfer from a rotating cylinder with and without crossflow. *ASME Trans.*, 1958, **80**, 70
14 General Electric Heat Transfer Division Manual, Rotating-surface convection cylinder without enclosure. Sec., 511.2, pp. 1–5, 1969
15 Jones, J. G. Mixed convection from a rotating horizontal heated cylinder placed in a low-speed wind tunnel. M.S. Thesis, University of Illinois at Chicago, 1987
16 Bejan, A. *Convection Heat Transfer*, Wiley, New York, 1985
17 Kreith, F. Convection heat transfer in rotating systems. In *Advances in Heat Transfer*, Vol. 5, Academic Press, New York, 1968
18 Poulikakos, D. and Bejan, A. The fluid dynamics of an attic space. *J. Fluid Mech.*, 1983, **131**, 251, 269
19 Patterson, J. and Imberger, J. Unsteady natural convection in a rectangular cavity. *J. Fluid Mech.*, 1980, **100**, 65–86
20 Fontan, A. and Lasek, A. Measure de faibles vitesse par un anemometer a fil chaud. *Rev. Generale Thermique*, 1970, **9**, 1159–1163

## Appendix

The key steps of the scaling analysis are as follows: the governing equations for boundary layer laminar mixed convection with respect to a curvilinear coordinate system measuring along ($x$) and perpendicular to ($y$) to the cylinder surface read

$$\frac{\partial u}{\partial x}+\frac{\partial v}{\partial y}=0 \tag{A1}$$

$$\frac{\partial}{\partial y}\left[u\frac{\partial u}{\partial x}+v\frac{\partial u}{\partial y}\right]-\frac{\partial}{\partial x}\left[u\frac{\partial v}{\partial x}+v\frac{\partial v}{\partial y}\right]$$
$$=\nu\left[\frac{\partial}{\partial y}\left(\frac{\partial^2 u}{\partial y^2}\right)-\frac{\partial}{\partial x}\left(\frac{\partial^2 v}{\partial y^2}\right)\right]-g\beta\sin\theta\frac{\partial T}{\partial y}+g\beta\cos\theta\frac{\partial T}{\partial x} \tag{A2}$$

$$u\frac{\partial T}{\partial x}+v\frac{\partial T}{\partial y}=\alpha\frac{\partial^2 T}{\partial y^2} \tag{A3}$$

Several explanations are needed for the momentum equation (A2). First, to obtain Equation A2, we cross-differentiate and subtract the two momentum equations (in the $x$- and $y$-directions) to eliminate the pressure terms. In addition, we adopt the usual Boussinesq approximation $\rho=\rho_\infty[1-\beta(T-T_\infty)]$ to relate the density in the body force terms of the momentum equations to temperature. The density was assumed to be constant everywhere else.

The momentum equation represents the combined effect of three mechanisms: inertia, friction, and buoyancy. For fluids with $\mathrm{Pr}\approx O(1)$ or greater, it has been shown[16,18,19] that the correct balance is between friction and buoyancy. This balance will be used in the present analysis. Next, the scales for the thermal boundary layer thickness will be obtained for three cases, in each of which a single heat transfer mechanism (free-stream forced convection, rotational forced convection, or natural convection) is dominant.

### *Thermal boundary layer thickness scale when free-stream forced convection dominates*

In this case, the appropriate scales for lengths and velocities are

$$x\sim\pi D/2,\quad y\sim\delta_{\mathrm{FC}},\quad u\sim U_\infty\sin\theta \tag{A4}$$

The scale for $v$ is obtained from Equations A4 and, with the help of the continuity equation (A1),

$$v\sim\frac{U_\infty\sin\theta}{D/2}\delta_{\mathrm{FC}} \tag{A5}$$

Scaling the energy equation based on the above yields

$$\frac{U_\infty\sin\theta}{\pi D/2}\Delta T\sim\frac{\alpha}{\delta_{\mathrm{FC}}^2}\Delta T \tag{A6}$$

Solving for the thermal boundary layer thickness and averaging over the cylinder surface, we obtain

$$\frac{\delta_{\mathrm{FC}}}{D}\sim\left[\frac{1}{\pi}\int_0^\pi\left(\frac{\pi}{2\sin\theta}\right)^{1/2}\mathrm{d}\theta\right]\mathrm{Pr}^{-1/2}\mathrm{Re}^{-1/2} \tag{A7}$$

The quantity in brackets in Equation A7 is evaluated numerically, resulting in a number whose magnitude is 0(1). Since our scaling analysis is correct in an order of magnitude sense, this number will be approximated by unity for simplicity. Therefore, the scale for the boundary layer thickness is

$$\delta_{\mathrm{FC}}/D\sim\mathrm{Re}^{-1/2}\mathrm{Pr}^{-1/2} \tag{A8}$$

### *Thermal boundary layer thickness scale when rotational forced convection dominates*

The analysis for this case is similar to what was described in the previous case. The main difference is that the velocity scales are

$$u\sim\omega\frac{D}{2},\qquad v\sim\omega\frac{D}{2}\frac{\delta_{\mathrm{RC}}}{\pi D/2} \tag{A9}$$

Proceeding as before, we obtain

$$\delta_{\mathrm{RC}}/D\sim\mathrm{Pr}^{-1/2}\mathrm{Re}_\omega^{-1/2} \tag{A10}$$

### *Thermal boundary layer thickness scale when natural convection dominates*

In this case, the scale for the $x$-component of velocity is obtained with the help of the momentum equation (A2). Balancing viscous and buoyancy forces in this equation yields

$$u\sim\frac{g\beta\Delta T}{\nu}\sin\theta\delta_{\mathrm{NC}}^2 \tag{A11}$$

Substituting this result into the continuity equation (A1), we obtain

$$v\sim\frac{g\beta\Delta T}{\nu}\sin\theta\frac{\delta_{\mathrm{NC}}^3}{\pi D/2} \tag{A12}$$

The remaining scales are analogous to those in the first case. Proceeding as before yields

$$\delta_{\mathrm{NC}}/D\sim\mathrm{Ra}^{-1/4}$$